J Mater Sci (2008) 43:2865–2868
DOI 10.1007/s10853-007-2088-6

Neutron-irradiation effects on track etching and optical characteristics of CR-39 (DOP) nuclear track detector

Puran C. Kalsi · Chhavi Agarwal

Received: 7 May 2007 / Accepted: 8 August 2007 / Published online: 25 September 2007

Abstract The effects of thermal neutron-irradiation in the neutron fluence range of (1.77–7.08) 10^{11} n/cm^2, on the etching and optical characteristics of diethylene glycol bis allyl carbonate (dioctyl phthalate doped), CR-39 (DOP) nuclear track detector have been studied using etching and UV–visible spectroscopic techniques. The bulk etch rates determined at different fluences were found to increase with an increase in neutron fluence up to 3.54×10^{11} n/cm^2, and then decrease at higher neutron fluence. The optical absorption spectra in the wavelength range of 200–800 nm were also recorded for the unirradiated and neutron irradiated samples in the above fluence range. The optical energy gaps (E_g) were determined by the shift in optical absorption edges as observed by UV–visible spectra of the neutron irradiated sample, using Tauc's expression. The UV–visible spectra results were further supported by determining the activation energies for bulk etching.

Introduction

The nuclear track detectors are extensively used in many accelerator and nuclear reactor-based studies. The structural and chemical damage of the detectors occur during the intense neutron, gamma and beta radiations in the reactor environment, which in turn affects the etching and optical characteristics of the detectors. Therefore, the effects of these radiations on the track etching and optical properties of nuclear track detectors are important for wider applications of these detectors. The effects of radiations such as gammas on the track etch rates and optical properties of nuclear track detectors have been extensively studied [1–8]. Only very few studies [9–12] have been carried out on neutron-induced effects. In addition to this, there is certainly a value in the exploration of neutron exposure of the polymers, to modify its property to be suitable for dosimeter applications. The neutrons themselves do not cause ionization directly. However, their secondary effects, in the form of recoiling atoms of the detector under neutron impact or the induction of nuclear reactions, lead to the production of charged particles that cause ionization [10]. In the present investigation, therefore, thermal neutron-irradiation effects on CR-39 (DOP) detector in the (1.77–7.08) 10^{11} n/cm^2 neutron fluence range are studied by UV–visible and bulk etch rate techniques. The optical absorption spectra for the neutron-irradiated detectors have also been recorded and using Tauc's plots, energy gaps were determined as a function of neutron fluence in the above range to study the optical changes induced by neutron-irradiation. The changes induced by neutron-irradiation were also studied by calculating the activation energy for bulk etching, determined from bulk etch rates at different temperatures.

Experimental details

CR-39 (DOP) sheets (thickness $\sim$ 330 μm) used in this study were manufactured by Pershore Moulding Ltd., UK, with 1% Dioctyl Phthalate.

Irradiation Facility and Sample irradiation: All samples of CR-39 (DOP) detectors were irradiated in the thermal column of the Apsara reactor, Trombay, Mumbai. Apsara is a swimming pool-type reactor. The wall of the pool is

P. C. Kalsi (✉) · C. Agarwal
Radiochemistry Division, BARC, Trombay, Mumbai 400085, India
e-mail: pckalsi@barc.gov.in

Table 1 Effects of thermal neutron fluence on the track etching and optical characteristics of CR-39 DOP) nuclear track detector

Neutron fluence (number of neutrons/cm^2)	V_b(μm/h)			Activation energy for bulk etching, E(eV)	E_g(eV)
	60 °C	70 °C	80 °C		
0	1.25	1.96	8.68	0.981 ± 0.001	3.88 ± 0.02
1.77×10^{11}	1.50	3.79	8.80	0.902 ± 0.039	3.81 ± 0.02
3.54×10^{11}	1.40	4.20	7.00	0.823 ± 0.019	3.79 ± 0.01
5.31×10^{11}	1.30	3.74	6.71	0.838 ± 0.014	3.83 ± 0.02
7.08×10^{11}	1.09	3.30	5.91	0.864 ± 0.016	3.85 ± 0.01

6-m-thick concrete. The thermal column is situated at one end of the pool with 2.5-m thick graphite. There is a beam hole of dimension 25 × 25 cm in the concrete wall. Samples were placed in an aluminium tray, which was moved into the thermal column. The thermal to epithermal neutron flux ratio of the thermal column is 5.6×10^3 which corresponds to a thermal neutron component of 99.98% [13]. The thermal neutron flux of the thermal column at the time of irradiation was also determined experimentally using the method reported from our laboratory [14], and was found to be 4.1×10^6 n/cm^2/s. The samples were irradiated at this neutron flux for 12, 24, 36 and 48 h. Hence the values of thermal neutron fluence (neutron flux × time of irradiation in second) for the irradiated CR-39 (DOP) detector samples in the present experiments were 1.77×10^{11}, 3.54×10^{11}, 5.31×10^{11} and 7.08×10^{11} n/cm^2. Since the CR-39 (DOP) detector is generally etched in 6N NaOH at 70 °C, the bulk etch rates, V_b of the unirradiated and the neutron irradiated detectors were determined at 70 °C using 6N NaOH as the etchant, by the loss in weight method [15]. In this method, a sample of the detector of known weight and surface area was dipped into the etchant solution, maintained at a fixed temperature in a thermostat, under conditions of stirring for an accurately noted time period. It was taken out, thoroughly washed with demineralized water, and was weighed again after air drying at room temperature. V_b was obtained in units of length per unit time as $V_b = m/2\ sdt$, where m is the weight loss due to etching for a time period t, s is the surface area and d is the density of the sample. The bulk etch rate values for different neutron fluences at 70 °C temperature and using 6N NaOH as the etchant, are given in Table 1. Each value is a mean of two determinations. The relative standard deviation on bulk etch rate values is about 5%. UV–visible spectra by a UV–VIS Spectrophotometer (Jasco, Model V-530) in the range of 200–800 nm of unirradiated and neutron irradiated samples of the detector, at different neutron fluences were also determined to study the changes induced in the detector by neutrons. To support the results obtained by UV–visible spectrophotometry, in addition to the bulk etch rates determined at 70 °C, the rates were also determined at 60 °C and 80 °C temperatures to deduce the activation energies for bulk etching.

Results and discussion

The bulk etch rates for the unirradiated and the neutron irradiated samples were determined by the method described above. Table 1 gives the values of bulk etch rate at 70 °C using 6N NaOH as the etchant for different neutron fluences. The V_b value at 70°C for the unirradiated detector is 1.96 μm/h. The bulk etch rate is seen to increase with the increase in the neutron fluence up to 3.54×10^{11} n /cm^2. At higher neutron fluence, the bulk etch rate has been found to decrease, as shown in Table 1. The interpretation of these results may be that up to the fluence 3.54×10^{11} n/cm^2 initial scission of the detector occurs forming free radicals. This is reflected by an increase in V_b values. At higher neutron fluence, the free radicals formed undergo cross-linking, which is indicated by a decrease in V_b values. The UV–visible spectra for the unirradiated and neutron irradiated CR-39 (DOP) samples were recorded and the 200–350 nm portions of them are shown in Fig. 1. The optical band gaps (E_g) were determined from the spectra using the Tauc's expression [7] $\omega^2 \epsilon_2 = [(h/2\pi)\omega - E_g]^2$ where ϵ_2 is the optical absorbance at wavelength λ. The absorption coefficient (ϵ_2) for different values of neutron fluence was determined. The values of $\sqrt{\epsilon_2}/\lambda$ were calculated and plotted against $1/\lambda$ on x-axis. The straight portion of the curve was then extrapolated and its intersection on the abscissa was determined [7]. This value corresponds to the inverse of the gap wavelength (λ_g). Figure 2 shows straight portion of the Tauc's plots for the unirradiated and the neutron irradiated CR-39 (DOP) samples. The band gap was then determined for the unirradiated and the neutron-irradiated samples using the relation h c/ λ_g. Table 1 contain the data on neutron dependent optical band gap (E_g). For UV–visible studies, triplicate measurements were done on each sample. Hence each E_g value is a mean of three determinations. It is clear from Table 1 that E_g values initially decrease up to neutron fluence of 3.54×10^{11} n/cm^2, and then increase at higher values of neutron fluence. The interpretation of these results can be that up to the neutron fluence of 3.54×10^{11} n/cm^2, in which the E_g values decrease, initial bond scission in the detector molecules is most

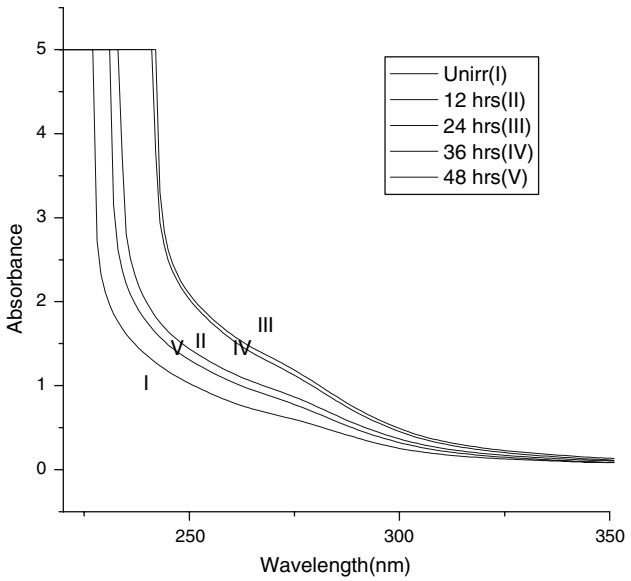

Fig. 1 UV–VIS spectra of unirradiated and thermal neutrons irradiated CR-39(DOP)

likely to occur. On the other hand, at higher neutron fluence, in which the E_g values increase, can be explained in terms of cross-linking.

To provide additional evidence to support the occurrence of chain scission and cross-linking seen by UV–visible studies at the above-mentioned fluences, the changes induced by neutron-irradiation were further studied by determining the activation energies for bulk etching. For this, bulk etch rates (V_b) for the unirradiated and the neutron irradiated detectors were also determined at 60 °C and 80 °C temperatures using 6N NaOH as etchant. The values of bulk etch rate at different temperatures are given in Table 1. In Fig. 3, we have plotted log V_b against the reciprocals of the absolute temperatures for the unirradiated and the neutron irradiated detectors. These plots confirm to the expression $V_b = A \cdot e^{-E/kT}$, where E is the activation energy for bulk etching, A is a constant for a given medium-etchant combination, k is Boltzmann constant and T is the temperature in K. The activation energy, E values for the unirradiated and the neutron-irradiated detectors are also given in Table 1. It is clear from the table that the activation energy values initially decrease up to neutron fluence of 3.54×10^{11} n/cm^2, and then increase at higher values of neutron fluence. These results also indicate that up to the neutron fluence of 3.54×10^{11} n/cm^2, in which the E values decrease, chain scission in the detector molecules is taking place. On the other hand, at higher neutron fluence the increase in E values can be explained in terms of cross-linking.

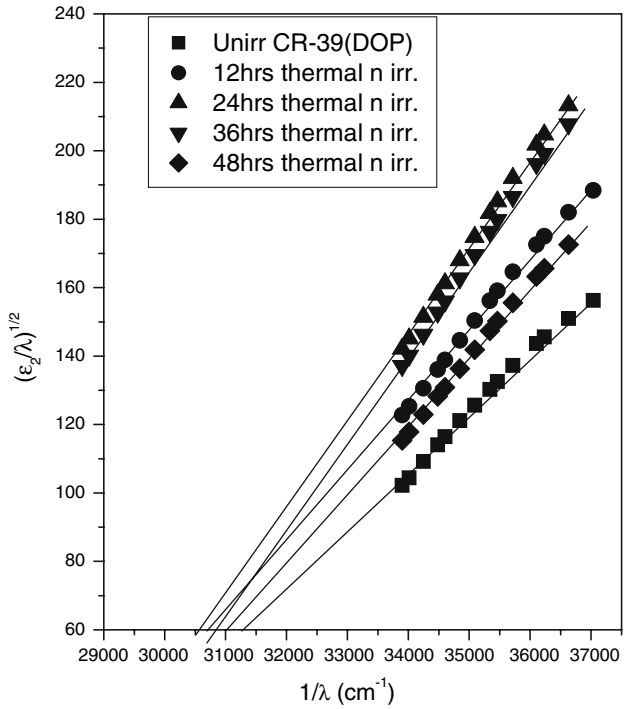

Fig. 2 Plot of $(\varepsilon_2/\lambda)^{1/2}$ versus $1/\lambda$, a representation of Tauc's relation to derive the optical band gap energy (E_g). The value of $\lambda_g^{-1}$was obtained by the extrapolation of the straight-line portion of the absorption edge to the $1/\lambda$ axis

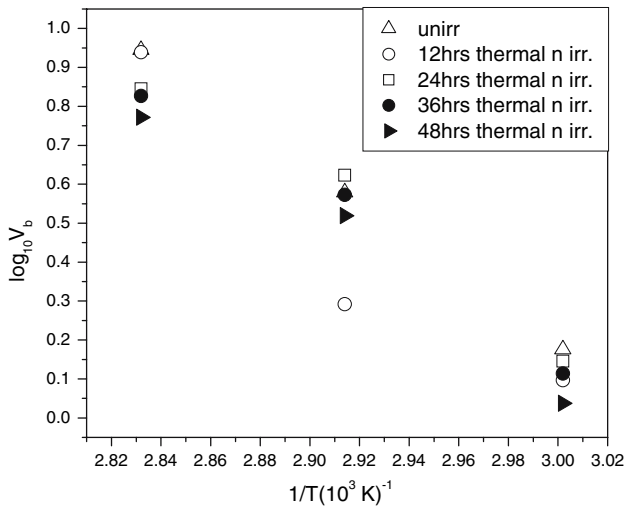

Fig. 3 Plot of $\log_{10} V_b$ versus 1/T for unirradiated and thermal n irradiated CR-39(DOP) detectors

Acknowledgement The authors are grateful to Dr. V. K. Manchanda, Head, Radiochemistry Division for his encouragement and support during this work.

References

1. Singh S, Prasher S (2005) Radiat Meas 40:50
2. Singh S, Prasher S (2004) Radiat Eff Defect S 159:359
3. Sinha D, Sahoo KL, Sinha UB, Swu T, Chemseddine A, Fink D (2004) Radiat Eff Defect S 159:587

4. Agarwal C, Kalsi PC, Ramaswami A (2006) Radiat Eff Defect S 161:131
5. Sharma T, Aggarwal S, Kumar S, Mittal VK, Kalsi PC, Manchanda VK (2007) J Mater Sci 42:1127
6. Singh S, Prasher S (2004) Nucl Instrum Meth B 222:518
7. Kulshreshtha SP, Sinha D, Mishra R, Tripathy SP, Dwivedi KK, Ghosh S, Fink D (2000) Radiat Meas 32:169
8. Buttafava A, Consolati G, Mariani M, Quasso F, Ravasio U (2005) Polym Degrad Stabil 89:133
9. Nouh SA, Abdel-Salam MH, Ahmed Morsy A (2003) Radiat Meas 37:25
10. Nouh SA, Hegazy TM (2006) Radiat Meas 41:17
11. Kalsi PC, Agarwal C (2007) Radiat Eff Defect S 162:25
12. Singh S, Sandhu AK, Prasher S, Pandey OP, Radiat Meas (In Press)
13. Nair AGC, Acharya R, Sudarshan K, Gangotra S, Reddy AVR, Manohar SB, Goswami A (2003) Anal Chem 75:4868
14. Iyer RH, Chaudhuri NK (1997) Radiat Meas 27:529
15. Kalsi PC (1999) J Radioanal Nucl Ch 242:169